Journal of Visualization, Vol. 7, No. 1 (2004) 85-92

Measurements of Aerodynamic Noise and Wake Flow Field in a Cooling Fan with Winglets

Nashimoto, A.*[1] *[2], Fujisawa, N.*[2], Akuto, T.*[3] and Nagase, Y.*[3]

*1 Mitsuba Corporation, 598, Minegishi, No, Niisato, Seta, Gunma, 376-0122, Japan.
*2 Department of Mechanical and Production Engineering Niigata University, 8050 Ikarashi 2, Niigata, 950-2181, Japan.
*3 Mitsuba Corporation, 1-2681, Hirosawa, Kiryu, Gunma, 376-8555, Japan.

Received 13 May 2003
Revised 18 August 2003

Abstract : The aerodynamic noise and the wake flow field in a cooling fan under actual operating conditions are studied with and without winglets on the fan blades. In order to understand the influence of the winglet, the aerodynamic noise and the wake velocity distribution are measured. The results indicated that overall noise level decreased and the noise spectrum was changed in a low frequency range when the winglet was installed. It was found from the flow visualization and PIV measurement that the influence of the winglet appeared in the traces of the tip vortices and the magnitude of vorticity was reduced in the near wake region, which suggest the observed reduction in aerodynamic noise.

Keywords : Aerodynamic noise, Flow visualization, PIV, Fan, Winglet, Tip vortex

1. Introduction

The noise generated from the cooling fan unit for automobiles is an important topic of interest in automobile engineering. The noise source from the fan unit can be categorized into mechanical and the aerodynamic noise. The former is caused by friction between the solid boundaries, but it can be considerably reduced by improvement in lubrication technology. Meanwhile, the latter comes from the aerodynamics of the blade itself, which becomes more important than the former with an increase in the rotational speed of the fan. In recent years, it has been required of motor vehicles to have highly-powered engines but with smaller compartments, so that the heat release from the radiator is increased, which leads to an increase in rotational speed of the cooling fan, too. Therefore, the study of reducing the aerodynamic noise from a cooling fan is becoming more and more important. Concerning this topic, Nashimoto et al. (2000) studied the shear-stress distribution over the suction side of the fan blade to understand the surface flow phenomenon on the blade, using an oil-film method combined with PIV analysis.

As one of the methods for reducing aerodynamic noise, the installation of winglets on the blade is reported to be effective by Dam (1984). However, the physical mechanism of the noise reduction by winglets has not been studied. This is because the measurements of the flow field around the rotating fan blade have not been conducted from the point of view of aerodynamic noise reduction. For this purpose, the particle image velocimetry (PIV) technique will provide an effective means for studying the structure of the wake flow field, because this technique is non-intrusive as well as a full

field measurement of the flow field.

In the present paper, the physical mechanism of noise reduction from a fan by installing a winglet on each blade is studied. To do this, the measurement of noise level and instantaneous velocity field around the blade are studied by using the phase-averaged PIV measurements.

2. Experimental Apparatus and Procedures

2.1 Experimental Setup

The experiment was carried out with a prototype fan used in a cooling fan unit for automobiles. The fan was located in combination with the shroud and the radiator to simulate the operating condition of the fan. Figure 1(a) is the schematic illustration of the experimental setup. All the components of the cooling fan unit, such as radiator, shroud, fan, and driving motor, were mounted on a stand. The fan was driven by an AC servo-motor and the fan speed was set at a constant speed with a controller.

Figure 1(b) shows the test fan with winglets. The winglet is installed on the suction surface of the blade. The fan is made of glass-filled plastics, having an outer diameter of 280 mm and the boss of 118 mm in diameter. The typical chord length is l=125 mm and the attack angle is 13°, which are measured at the radial position r = 140 mm. The fan has four blades and the blade pitch is made slightly irregular to reduce the noise that depends on fan speed and the number of blades. The proper height and attachment position of winglets to reduce aerodynamic noise were studied and found to be 15 mm and 10 mm from the blade tip, respectively, through preliminary experiments. The tip clearance made by fan and shroud is 3.5 mm. The details of the winglet viewed from the suction side of the blade are given in Fig.1(c). Note that the airflow rate and the static pressure at the design condition are 941 m³/s and 82 Pa, respectively, in the case of without winglts and 928 m³/s and 79 Pa, respectively, in the case of with winglets.

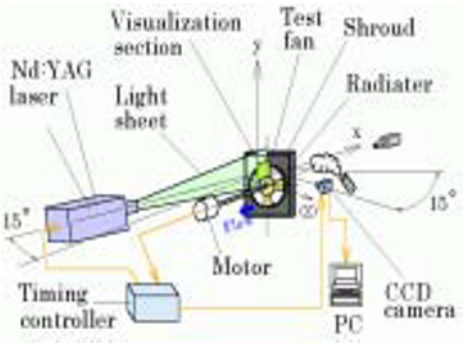

(a) Experimental apparatus

(b) Geometry of test fan (view from pressure side)

(c) Winglet on blade (view A)

Fig. 1. Experimental apparatus and measurement system.

2.2 Noise Measurement

The sound pressure level *SPL*(dB) in the present experiment was measured with a sound level meter located 1m in front of the radiator. The noise measurement was conducted in an anechoic chamber. The background noise in the chamber was smaller than 20 dB. The noise level was obtained from the noise measurement with A-weighted filter. The frequency spectrum was obtained by using the FFT analyzer. The test fan was selected from the same lot of product to minimize the geometrical effect of the fan blade on the noise measurement. The fan without winglets was prepared by cutting off the winglets and smoothed out the surface. The maximum difference of noise level in the same production lot was found to be smaller than 0.2 dB. Although the rotational speed N of the fan was varied in the present experiment, the main experimental study was carried out at the design

condition N = 2300 rpm, so that the Reynolds number R_e (= $V_t r / \nu$) = 3.1 × 10^5, where r is a radius of the fan blade tip, V_t is a blade tip velocity and ν is a kinematic viscosity of fluid air (=1.5 × 10^{-5} m^2/s).

2.3 Flow Visualization and PIV Measurement

Flow visualization and PIV measurement were conducted with the same experimental conditions as the noise measurement. The smoke tracer particles were supplied from the nozzle of a smoke generator, which was set at 0.5 m upstream from the radiator. The diameter of the smoke particle is about 1μm. Illumination was provided from a double pulsed Nd:YAG laser (30 mJ/shot) to visualize the cross-sectional view in the wake of the fan, where the light sheet was about 1 mm in thickness. The visualized images were taken by a monochrome CCD camera with 8 bits having a spatial resolution of 960(H) × 1018(V) pixels. Details of the measurement technique by PIV are described by Tomimatsu et al. (2002). For image photography of vortex cross-section (x-y plane in Fig. 1(a)), the light sheet was inclined by 15° against the motor shaft (x-axis) to see the development of the vortices in the wake and the CCD camera was set at right angles to the light sheet plane as shown in Fig. 1(a). (Note that the vortices from the fan blade develop at 10°-18° against the radiator surface, which will be described in the following section.)

When the position signal of the motor is input into the timing controller, the controller outputs the pulse signals to the CCD camera and the lasers. Therefore, two images are captured in a short time interval at a fixed angle of fan blade. The time delay between the position signal of the motor and the laser illumination was found to be less than 1 μs, which is negligibly small in the present experiment. In order to obtain a phase-averaged velocity field by PIV, 160 images (80 sets) were captured at a fixed angle of fan blade. The spatial resolution of each image was 66 μm/pixel, the interval between two images was 10 μs, and the maximum particle displacement was 7 pixels. The images of the tip vortex were captured at angles between θ 60° and 170° at every interval of 10°, where the angle θ is measured from the leading edge of the blade as defined in Fig. 1(b).

The PIV analysis was carried out under the conditions of an interrogation window size of 32 × 32 pixels and with 50% area overlap. The analyzed result showed erroneous vectors less than 1% of the total number of velocity vectors, which were eliminated by comparing with the surrounding velocity vectors. It is to be noted that the uncertainty interval of the measurement is estimated to be 3% with 95% confidence, which is based on the uncertainty analysis by Kobayashi et al. (2002). The vorticity ζ (= r/V_t ($\partial V/\partial x$ - $\partial U/\partial y$)) in the flow field was evaluated from the velocity distribution, where r (= 140 mm) indicates the radius of fan blade tip, V_t (= 33.7 m/s) the peripheral velocity at the blade tip, and U and V are the velocity components in x and y directions, respectively.

3. Results and Discussions

3.1 Noise Characteristics

Figure 2(a) gives the overall sound pressure level SPLo(dB) of the test fan with and without winglets, which are measured at the rotational speed ranging from 2150 to 2450 rpm, which covers the design condition of the fan at 2300 rpm. The result shows that the noise level of the fan increases with an increase in rotational speed in both fans with and without winglets, without any peaks in the noise level. It is also found that the noise level of the winglet fan is generally smaller than that without winglets with a reduction in noise level about 1 dB. This result indicates an effectiveness of the winglet for the reduction of noise from the fan. The uncertainty interval of noise measurement was 0.2 dB at 95 % coverage. However, the measured airflow rate was decreased by 1.5% in the fan with winglets, so that the actual noise reduction can be estimated as 0.7 dB by considering the influence of the airflow velocity with using the acoustic similarity law for fan (Adachi et al. 1997). Note that efficiency of the fan is decreased by 0.6 % by the installing of the winglet.

Figure 2(b) shows the spectrum of the noise SPL(dB) with and without winglets, which are

measured at a rotational speed of 2300 rpm at the design condition. Since the deviations in the measurements with and without winglets are rather small, the subtracted result is also shown. The result indicates that the noise spectrum with winglets decreased in the frequency range smaller than 6 kHz in comparison to the case without winglets. Therefore, the observed reduction in the noise level is attributed to the change of the spectrum at low frequency range.

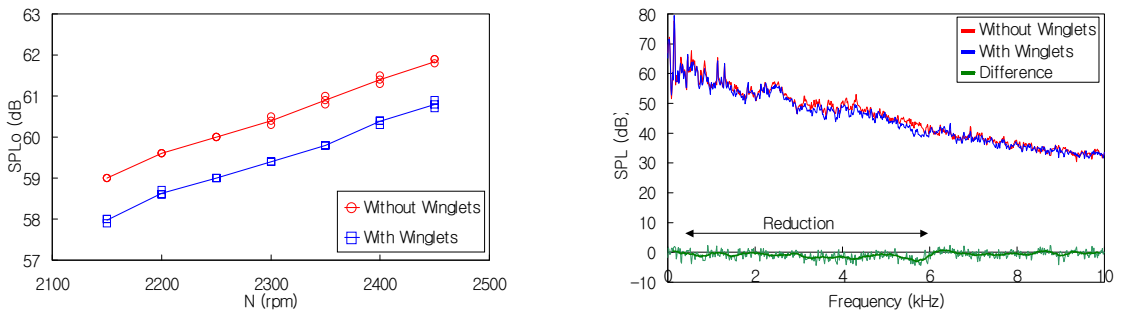

(a) Overall sound pressure level (b) Noise spectrum

Fig. 2. Overall sound pressure level and spectrum.

3.2 Visualization of Vortex Structure

Figures 3 and 4 show the smoke visualization images of the flow field generated from the rotating blade with and without winglet, respectively, at the design condition 2300 rpm. The results are given at every 10° from θ = 60° to 150° of the rotor angle measured from the leading edge of the blade. It is to be noted that the images are taken from the downstream side of the blade, which is illustrated on the left hand side of the images. It is also to be noted that the image at θ = 60° represents the flow field when the trailing edge of the blade has just passed through the light sheet plane. The visualization of the flow field without winglets (Fig. 3) shows the presence of two black spots, which correspond to the vortex cores of the tip vortices generated from the blades. It is expected that the smoke particles in these areas move to the radial direction due to the centrifugal forces of the generated vortices. It is to be mentioned that the vortex core on the right side is just generated from the suction side of the blade, while that on the left side is produced from the suction side of the preceding blade. Therefore, the position of the vortex core shifts to the axial direction slightly inclined to the inside. It is found from the PIV measurement, which will be described in the next section, that these vortices are whirling in a clockwise direction. As the blade rotates, i.e., as the angle θ becomes larger, these vortices move to the axial direction (to the left on the figure), and in the image at θ = 110°, the following blade is recognized on the right hand side of the image. Then, the new vortex appears in the wake of the blade at θ = 150°, which is just a blade after the image at θ = 60°. Therefore, the flow structure at θ =150° is very similar to the observation at θ = 60°, which also indicates the repeatability of the flow pattern in the wake at every θ = 90°.

On the other hand, the observation of the flow field with winglets indicates the change of the vortex structure in the wake flow field, which is shown in Fig. 4. At the rotor angle θ = 60°, that is just downstream of the passing blade, two vortices are generated from the suction side of the blade. The upper vortex near the shroud is rotating in a clockwise direction similar to the observation without winglets. However, the size of the vortex core looks smaller than that without winglets. On the other hand, the vortex on the lower side is generated by the influence of winglets, which is whirling in the same direction as the tip vortices. This winglet vortex moves in the axial direction faster than the tip vortex with an increase in rotor angle from θ = 60° to 90°. However, the winglet vortex disappears at larger rotor angle than θ = 100° until the new winglet vortex appears at θ = 150°, which is one cycle after the passing blade. Therefore, the traces of the winglet vortex are not observed on the left side of the blade. It is to be noted that the size of vortex core is also reduced in

this region in comparison with the case without winglets. Further quantitative discussion on the vortices will be given in the next section.

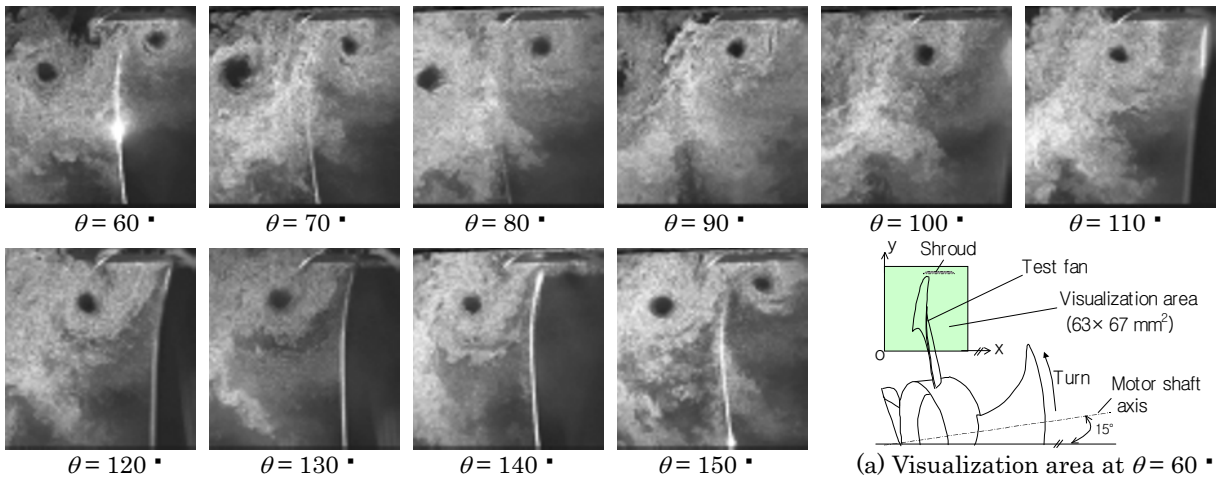

Fig. 3. Smoke visualization of the fan wake without winglet.

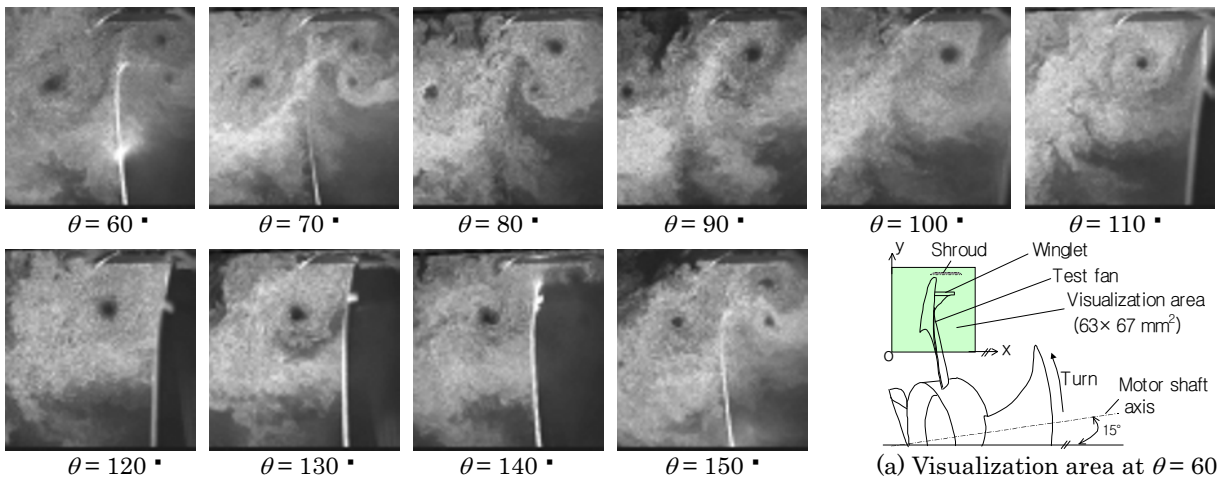

Fig. 4. Smoke visualization of the fan wake with winglet.

3.3 Phase Averaged Velocity and Vorticity Distribution

The visualization images are analyzed by cross-correlation algorithm to measure the instantaneous velocity distributions at a fixed rotor angle, which are averaged over to obtain the contours of phase-averaged velocity magnitude $\sqrt{U^2 + V^2}$ and the vorticity ζ. Typical examples of phase-averaged velocity magnitude and vorticity contour are shown in Figs. 5 and 6, respectively, at three rotor angle θ= 70°, 100°, and 130° without the winglets on the blades. Since the flow pattern is repeatable at the same rotor angle, the phase-averaging procedure is well suited for the analysis of the wake flow field of the fan blade. The phase-averaged velocity distribution shows the large velocity gradient on both sides of the rotating blade, which corresponds to the generation of negative vorticity as shown in Fig. 6. The position of the negative vorticity matches well with the black spot in the visualized image in Fig. 3. As the rotor angle increases from θ= 70° to 130°, the velocity magnitude around the vortices decreases and the magnitude of the vorticity reduces, which indicate the diffusion of the tip vortex generated from the leading edge of the blade due to the turbulent diffusion of the flow.

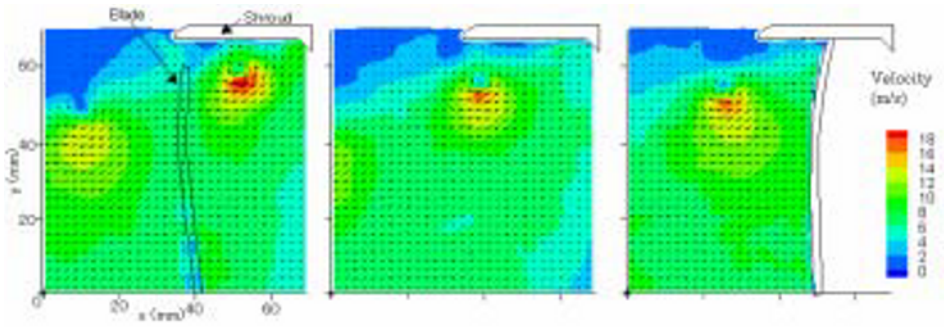

$\theta = 70°$ $\theta = 100°$ $\theta = 130°$

Fig. 5. Phase-averaged velocity distribution of fan wake without winglet.

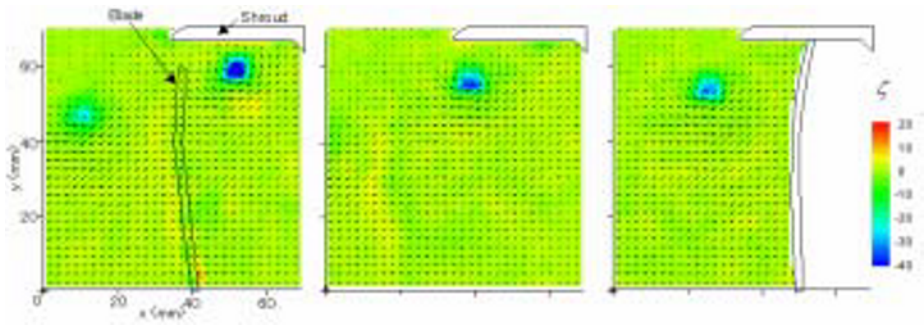

$\theta = 70°$ $\theta = 100°$ $\theta = 130°$

Fig. 6. Vorticity distribution of fan wake without winglet.

When the winglets are placed on the blades, the velocity and vorticity distributions are modified as shown in Figs. 7 and 8, respectively. These distributions show the presence of three vortices in the wake flow field, which agrees with the smoke visualization image in Fig. 4. It is found that the tip vortex at the upper right of the distribution shows the negative vorticity and moves to the axial direction with an increase in the rotor angle, which is similar to the case without winglets. But, the moving velocity of the tip vortex is smaller than the case without winglets, which may be due to the interaction of the tip vortex with the winglet vortex on the lower side. The winglet vortex also indicates the negative vorticity, but the magnitude is much smaller than the tip vortex. The distance between the vortices seems to be increased with an increase in the rotor angle.

It is expected that the winglet vortex is generated by the interaction of the flow with the winglets, because the generated vortex is close the winglet. It should be mentioned that the magnitude of the vorticity of the tip vortex is weakened about 10% at $\theta = 70$ by the presence of the winglet, which suggests the reduction of aerodynamic noise by the influence of the winglets.

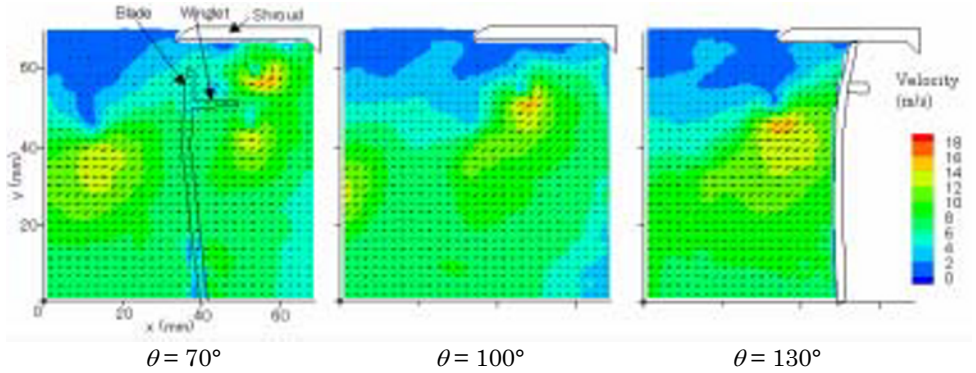

$\theta = 70°$ $\theta = 100°$ $\theta = 130°$

Fig. 7. Phase-averaged velocity distribution of fan wake with winglet.

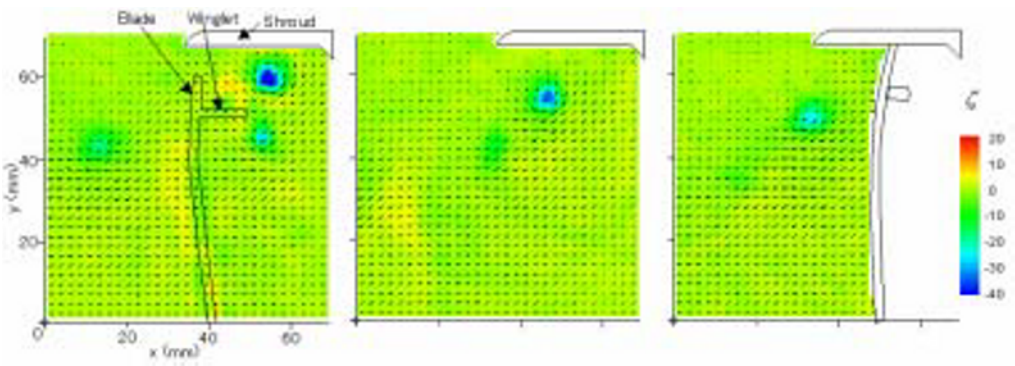

$\theta = 70°$ $\theta = 100°$ $\theta = 130°$

Fig. 8. Vorticity distribution of fan wake with winglet.

3.4 Iso-Vorticity Contours of Vortex Structure

In order to understand the development of the vortices in the fan wake, the iso-vorticity contours are visualized in three-dimensional space, which is shown in Fig. 9. They are obtained from the cross-sectional vorticity distribution at every 10° in rotor angle ranging from θ = 60° to 170° and the contour surfaces are visualized at constant vorticity $\zeta = -12$. It is to be noted that the contour surface has the locally high vorticity in the wake flow field and corresponds to the vortex traces. As can be seen in the contour plot without winglets in Fig. 9(a), the traces of the vorticity are generated from the suction side of rotating blades and develop to the peripheral direction, but incline 12° to the axial direction. Similar vorticity traces were obtained without the shroud of a fan by Cai et al. (2002) by analyzing the velocity data from the LDV measurements.

When the winglets are installed on the blades, the vortex traces are modified as shown in Fig. 9(b). There are two vortex traces formed in the wake of the blade, one is the tip-vortex and the other is the winglet vortex. Both the vortices leave from each other near the wake region of the blade. It was found that the vortex angle is slightly decreased to 10 by installing the winglet. This change of vortex angle is due to the occurrence of winglet vortex, which develops at the vortex angle 18 and the magnitude of the vorticity becomes small in the wake of the blade. Therefore, the tip vortex and the winlet vortex seems to develop apart from each other, which may be due to the repelling forces of corotating vortices in the flow field. It is to be noted that the diameter of the contour surface is reduced by the installation of winglet, which corresponds to the reduction of the vorticity in the fan with winglet. Such changes of the tip vorticity will contribute to the reduction in aerodynamic noise.

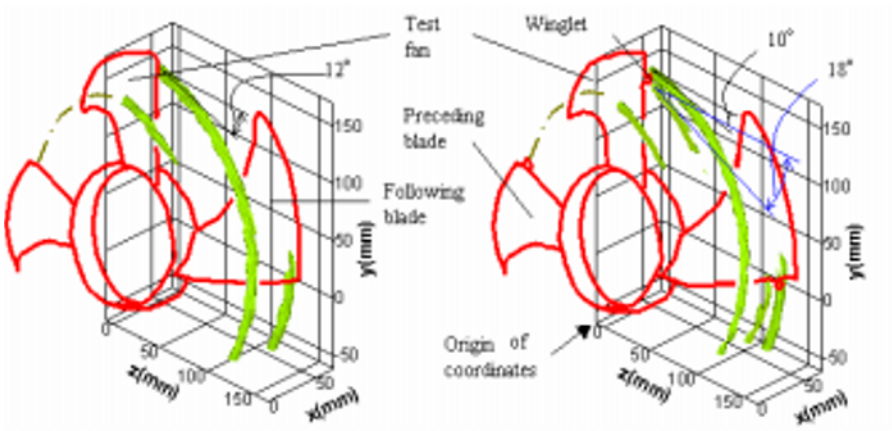

(a) Without winglet (b) With winglet

Fig. 9. Iso-vorticity contours of vortex traces.

4. Conclusion

The aerodynamic noise and the flow field of a cooling fan under actual operating conditions were studied with and without winglets on the fan blades to understand the influence of winglets.

The measurement of aerodynamic noise from the fan indicated that the overall noise level of the fan blades with winglets was smaller than that without winglets, which is due to the change of the noise spectrum in a lower frequency range.

In order to understand the mechanism of noise reduction, the wake flow field was visualized by a smoke injection technique. The visualization result showed the creation of a winglet vortex in the wake of the blade, which modifies the development of the tip-vortex generated from the leading edge of the suction side of the blade. The interaction of these vortices was quantitatively visualized using the phase-averaged velocity and vorticity distributions, which are obtained from the PIV measurement. It was also found that the trace of tip-vortex was modified and the vorticity was reduced by the influence of winglet vortex. Therefore, the aerodynamic noise generated from the tip vortex is expected to be reduced by the influence of the winglets installed on the blades.

References

Cai, W. X., Shiomi, N., Sasaki, K., Kaneko, K. and Setoguchi, T., Visualization of Tip Vortex Flow in an Open Axial Fan by EFD, Journal of Visualization, 5-3 (2002), 293-300.

C. P. van Dam, Natural Laminar Flow Airfoil Design Considerations for Winglets on Low-Speed Airplanes, NASA Contract Report, NASA-CR-3853, (1984), 1-28.

Kobayashi, T. et al., Handbook of Particle Image Velocimetry (First edition), (2002), 151-162, Morikita, Tokyo(in Japanese).

Nashimoto, A., Fujisawa, N., Kimura, E. and Akuto, T., Visualization of Surface Flow over a Blade of Rotating Machinery by Oil-Film Technique and Measurement of Shear Stress Distribution by Image Analysis, Journal of The Visualization Society of Japan, 20-79 (2000), 56-61(in Japanese).

Tomimatsu, S., Fujisawa, N. and Hosokawa, A., Measurement of Aerodynamic Noise and Unsteady Flow around a Symmetrical Airfoil, Journal of Visualization, 5-4 (2002), 381-388.

Adachi, I. et al., JSME Mechanical Engineers' Handbook; Applications; Fluid Mechinery (First edition), (1997), 26-27, Maruzen, Tokyo (in Japanese).

Author Profile

Atsushi Nashimoto: After graduating from Kiryu technical high school in 1972, he joined Mitsuba Corporation in 1972 working in the Production Engineering Department from 1972 to 1978, and in the Research Department from 1978 to 1996. Since 1996, he has been engaged in the Technical Development Department and working in the field of flow visualization of rotating machinery. Now he is a Ph.D. student of Niigata University.

Nobuyuki Fujisawa: After graduating from Tohoku University (D.E. 1983), he joined Gunma University in 1983 and worked as an associate professor in 1991. Since 1997, he has been a professor of Niigata University and is continuing research on the visualization and non-intrusive measurement technique of velocity, temperature and shear stress in mechanical engineering.

Tsuneo Akuto: After graduating from Keio University (M.S.) in March 1971, he joined Japan INS. He later joined Mitsuba Corporation in August 1971, working in the Production Engineering Department from 1971 to 1972, Quality Control Department from 1972 to 1975 and Research Department from 1975 to 1994. Since 1994, he has been engaged in management of the Development Departments.

Yuichi Nagase: After graduating from Meiji University in 1976, he joined Mitsuba Corporation and worked in the Quality Control Department from 1976 to 1987, Experimental Department from 1987 to 1992 and Electronic Engineering Department from 1992 to 1998. Since 1998, he has been engaged in management of the Technical Development Department.